Quantum Zeno and anti-Zeno effects in open quantum systems

Zixian Zhou,[1,2,*] Zhiguo Lü,[1,2,†] Hang Zheng,[1,2,‡] and Hsi-Sheng Goan[3,4,§]

[1]*Key Laboratory of Artificial Structures and Quantum Control (Ministry of Education), Department of Physics and Astronomy,*
Shanghai Jiao Tong University, Shanghai 200240, China
[2]*Collaborative Innovation Center of Advanced Microstructures, Nanjing University, Nanjing 210093, China*
[3]*Department of Physics and Center for Theoretical Sciences, National Taiwan University, Taipei 10617, Taiwan*
[4]*Center for Quantum Science and Engineering, National Taiwan University, Taipei 10617, Taiwan*

The traditional approach to the quantum Zeno effect (QZE) and quantum anti-Zeno effect (QAZE) in open quantum systems (implicitly) assumes that the bath (environment) state returns to its original state after each instantaneous projective measurement on the system and thus ignores the cross-correlations of the bath operators between different Zeno intervals. However, this assumption is not generally true, especially for a bath with a considerably nonnegligible memory effect and for a system repeatedly projected into an initial general superposition state. We find that, in stark contrast to the result of a constant value found in the traditional approach, the scaled average decay rate in unit Zeno interval of the survival probability is generally time dependent or shows an oscillatory behavior. In the case of a strong bath correlation, the transition between the QZE and the QAZE depends sensitively on the number of measurements N. For a fixed N, a QZE region predicted by the traditional approach may in fact already be in the QAZE region. We illustrate our findings using an exactly solvable open qubit system model with a Lorentzian bath spectral density, which is directly related to realistic circuit cavity quantum electrodynamics systems. Thus the results and dynamics presented here can be verified with current superconducting circuit technology.

I. INTRODUCTION

With the development of quantum information and computation, the quantum Zeno effect (QZE) [1–4] has attracted much attention as one of the means to prolong the quantum coherence of an open quantum system against the influence of its surrounding environment (bath) [5–7]. Another significant effect in open quantum systems, the quantum anti-Zeno effect (QAZE)—i.e., if the repeated measurements are not rapid enough, the measurements may actually enhance the quantum transitions—was revealed by Kofman and Kurizki [8–10]. Each of the repeated measurements on the system of interest in most studies is considered as an ideal, instantaneous, projective measurement. Even so, the traditional Kofman and Kurizki approach (KKA) to the QZE and QAZE for open quantum systems (implicitly) assumes that the bath state returns to its original state after each instantaneous projective measurement on the system [11–22]. Consequently, the survival probability (SP) $P_{\text{KKA}}(t)$ that the system is still in its initial state $|\psi_S\rangle$ after N repeated measurements with equal time interval τ is written as

$$P_{\text{KKA}}(t) = [P_{\text{KKA}}(\tau)]^N$$
$$= \{\text{Tr}_{S \otimes B}[\mathcal{P}_S U(\tau)\rho_{\text{tot}}(0)U^\dagger(\tau)\mathcal{P}_S]\}^N, \quad (1)$$

where time $t = N\tau$, $P_{\text{KKA}}(\tau)$ is the SP in the initial state right after a single measurement is performed ($N = 1$) [23], $\mathcal{P}_S = |\psi_S\rangle\langle\psi_S|$ is the system state projector, $\rho_{\text{tot}}(0) = \mathcal{P}_S \otimes \rho_B(0)$ is the initial system-bath state, $U(\tau)$ is the evolution operator

of the total system-bath Hamiltonian, and $\text{Tr}_{S \otimes B}$ denotes a trace taken over the degrees of freedoms of the system and bath. However, this assumption of the KKA is not always valid.

For a general case, the bath state changes throughout the process. The SP in a general approach (GA) should be

$$P(t) = \text{Tr}_{S \otimes B}\{[\mathcal{P}_S U(\tau)]^N \rho_{\text{tot}}(0)[U^\dagger(\tau)\mathcal{P}_S]^N\}, \quad (2)$$

i.e., the trace over the system and bath variables is performed at the end of the measurements rather than after each measurement as in the KKA. In other words, the SP $P_{\text{KKA}}(t)$ in the KKA is just the Nth power of the SP $P_{\text{KKA}}(\tau)$ and thus neglects the cross-correlation of the bath operators between different Zeno intervals [11–22]. This yields significantly quantitatively and qualitatively different predictions in QZE and QAZE behaviors between the KKA and the GA, especially when the repeated measurements project the system into an initial general superposition state (not just in an initial single excited eigenstate) and when the bath has a considerably nonnegligible memory effect. It is the aim of this paper to unveil these important differences. The key qualitative differences we find are as follows. The average decay rate in each Zeno interval is constant in the KKA, while it is time dependent in the GA. In the regime of very small Zeno intervals, the SP shows exponential-decay behavior in the KKA, but the SP in the GA can exhibit nonexponential decay. The total average decay rate depends only on the Zeno interval τ in the KKA, while it also depends on the number of repeated measurement N in the GA. Thus previous studies on QZE-QAZE transitions [11–13] for non-Markovian open quantum systems using the properties of the total average decay rates need to be reexamined.

*zzx1313@sjtu.edu.cn
†zglv@sjtu.edu.cn
‡hzheng@sjtu.edu.cn
§goan@phys.ntu.edu.tw

II. MODEL AND DYNAMICS

We illustrate our results through a qubit system interacting with a bath that has a nonnegligible bath correlation (memory) time [24,25]. The total Hamiltonian without making the rotating-wave (RW) approximation in the system-bath coupling reads

$$H_{\text{tot}} = \frac{\Delta}{2}\sigma_z + \sum_k \omega_k b_k^\dagger b_k + g\sigma_x \sum_k \mu_k(b_k + b_k^\dagger), \quad (3)$$

where $\sigma_{x,z}$ are the Pauli operators, b_k ($b_k^\dagger$) is the bath annihilation (creation) operator for bath mode k, and Δ and g are the qubit frequency and coupling constant, respectively. We choose the bath spectral density in a Lorentzian form,

$$J(\omega) = \sum_k |\mu_k|^2 \delta(\omega_k - \omega) \quad (4)$$

$$= \frac{\Gamma}{\pi} \frac{1}{(\omega - \omega_0)^2 + \Gamma^2}, \quad (5)$$

with width Γ, central frequency ω_0, and normalization condition $\sum_k \mu_k^2 = 1$. This not only relates our model directly to a realistic circuit cavity quantum electrodynamics (QED) system [18,19,26–31], but also allows a well-defined bath correlation time $1/\Gamma$ to characterize the memory effect of the bath. Besides, we choose the initial density matrix for the bath as $\rho_B(0) = |0_B\rangle\langle 0_B|$ with bath vacuum $|0_B\rangle$. The Lorentzian bath initially in the vacuum state $|0_B\rangle$ at zero temperature makes the spin-boson model with any bilinear form of qubit-bath coupling (with or without the RW approximation) exactly solvable [32–34].

A. Bath representation

We describe next how to obtain an exact evolution equation for the spin-boson model with a Lorentzian spectral density and any bilinear form of qubit-bath coupling. First, we discuss how a bath (with many or infinite degrees of freedom) having a Lorentzian spectral density can be represented as a single bosonic mode coupling with an interacting Hamiltonian in an RW form to a fictitious white reservoir [34,35]. We show that this representation or decomposition is not an approximation of the original bath model but rather is exact for a bath state initially in the vacuum state $|0_B\rangle$ at zero temperature. Consider the qubit-bath (spin-boson) model of Eq. (3) in which no RW approximation is made onto the qubit-bath coupling Hamiltonian. Suppose we express the bath Hamiltonian, consisting of a collection of an infinite number of harmonic oscillators, as

$$\sum_k \omega_k b_k^\dagger b_k = \omega_0 a^\dagger a + \sum_q \Omega_q d_q^\dagger d_q + a^\dagger \sum_q \gamma_q d_q$$
$$+ a \sum_q \gamma_q^* d_q^\dagger, \quad (6)$$

where a is the annihilation operator of a single bosonic mode with characterized frequency ω_0, d_q is the annihilation operator of a reservoir mode q with frequency Ω_q, and γ_q is the coupling strength between the single mode and the reservoir mode q. We may regard the original bath operators b_k as the normal modes of the right-hand-side quadratic RW coupling model.

To make this decomposition clearer, let us rewrite the bath Hamiltonian, Eq. (6), considering the continuous spectrum of excitations in the bath. Making use of the transformation between the discrete boson operators d_q and the continuous ones d_Ω,

$$d_q = \sqrt{D(\Omega_q)} \int_{1/D(\Omega_q)} d\Omega\, d_\Omega, \quad (7)$$

and a similar transformation between the discrete operators b_k and continuous ones b_ω, where $D(\Omega_q)d\Omega_q$ is the number of modes in the reservoir with frequencies between Ω_q and $\Omega_q + d\Omega_q$, and $\int_{1/D(\Omega_q)} d\Omega$ represents an integration in a band of width $1/D(\Omega_q)$ around Ω_q [35], one obtains

$$\int \omega b_\omega^\dagger b_\omega d\omega = \omega_0 a^\dagger a + \int \Omega d_\Omega^\dagger d_\Omega d\Omega$$
$$+ a^\dagger \int \nu_\Omega d_\Omega d\Omega + a \int \nu_\Omega^* d_\Omega^\dagger d\Omega, \quad (8)$$

where $\nu_\Omega = \sqrt{D(\Omega)}\gamma_\Omega$, γ_Ω denotes the corresponding quantity of γ_q in the continuous spectrum representation, and the integral $\int d\Omega = \sum_q \int_{1/D(\Omega_q)} d\Omega$ covers the whole spectrum of excitations of the reservoir [35]. It has been shown in Ref. [35] that the Hamiltonian on the right-hand side of Eq. (8) can be diagonalized and the normal modes b_ω satisfying $[b_\omega, b_{\omega'}^\dagger] = \delta(\omega - \omega')$ can be expressed as

$$b_\omega = \xi_\omega a + \int \eta_{\omega,\Omega} d_\Omega d\Omega, \quad (9)$$

where ξ_ω and $\eta_{\omega,\Omega}$ satisfy the following equations:

$$|\xi_\omega|^2 = \frac{|\nu_\omega|^2}{[\omega - \omega_0 - F(\omega)]^2 + [\pi|\nu_\omega|^2]^2}, \quad (10)$$

$$\eta_{\omega,\Omega} = \left[P\frac{1}{\omega - \Omega} + \frac{\omega - \omega_0 - F(\omega)}{|\nu_\omega|^2}\delta(\omega - \Omega) \right] \nu_\Omega \xi_\omega, \quad (11)$$

where P denotes the principal part in the integral, and

$$F(\omega) = P \int \frac{|\nu_\Omega|^2}{\omega - \Omega} d\Omega. \quad (12)$$

Furthermore, the single mode a can be reexpressed by the normal modes as

$$a = \int f_\omega b_\omega d\omega. \quad (13)$$

The coefficient f_ω can be determined as follows. Substituting Eq. (13) for a into the commutator $[a, b_\omega^\dagger]$, one obtains $[a, b_\omega^\dagger] = f_\omega$; then substituting Eq. (9) for b_ω into the same commutator, one obtains $[a, b_\omega^\dagger] = \xi_\omega^*$. Thus one concludes that the coefficient $f_\omega = \xi_\omega^*$. The above equations for the diagonalization are all exact and independent of the expression or form of the spectral density of the reservoir d_Ω. Now, suppose the reservoir is white, i.e., the spectral density

$$G(\Omega) = |\nu_\Omega|^2$$
$$\equiv \sum_q |\gamma_q|^2 \delta(\Omega - \Omega_q)$$
$$= \Gamma/\pi; \quad (14)$$

then one can easily obtain from Eqs. (12) and (10) that $F(\omega) = 0$ and thus

$$|\xi_\omega|^2 = \frac{\Gamma}{\pi} \frac{1}{(\omega - \omega_0)^2 + \Gamma^2}, \tag{15}$$

which is the same Lorentzian form as the spectral density $J(\omega)$ of Eq. (5) of the original bath. Consequently, one can, by making use of Eq. (13) with the relation $f_\omega = \xi_\omega^*$ and Eqs. (4) and (5), rewrite the single mode in terms of the normal modes in the discrete form as

$$a = \sum_k \mu_k b_k, \tag{16}$$

where b_k and μ_k are the original bath annihilation operator and qubit-bath coupling strength, respectively. Furthermore, the commutation relation $[\sum_k \mu_k b_k, \sum_k \mu_k b_k^\dagger] = \sum_k \mu_k^2 = 1$ confirms once again the relation of Eq. (16). Expressing the original bath modes in the total Hamiltonian, (3), in terms of the single mode a and the white reservoir modes d_q, one obtains

$$H_{\text{tot}} = \frac{\Delta}{2}\sigma_z + g\sigma_x(a + a^\dagger) + \omega_0 a^\dagger a + \sum_q \Omega_q d_q^\dagger d_q$$
$$+ a^\dagger \sum_q \gamma_q d_q + a \sum_q \gamma_q d_q^\dagger, \tag{17}$$

where the spectral density of the white reservoir is given by Eq. (14). Thus treating the original Lorentzian bath as a single mode coupled to a flat white reservoir (flat continuum) in an RW form is an exact result.

B. Exact master equation

The correlation function of the white-reservoir operators reads

$$\alpha(t,s) = \sum_q |\gamma_q|^2 e^{-i\Omega_q(t-s)}$$
$$= \int G(\Omega) e^{-i\Omega(t-s)} d\Omega$$
$$= \Gamma \delta(t - s), \tag{18}$$

that is, the white reservoir correlation time $\tau_R \to 0$ is treated as the shortest time scale in the problem. So the degrees of freedom of the white reservoir can be traced out first regardless of the repeated projections of the system or the form of the system-bath interaction.

The master equation for the reduced density matrix of a single bosonic mode (or a harmonic oscillator) coupled to a reservoir (bath) through an RW-type coupling Hamiltonian can be obtained exactly for an arbitrary bath spectral density (or bath correlation function) and for an initial zero-temperature equilibrium reservoir vacuum state [36] or an initial finite-temperature thermal equilibrium reservoir state [37]. We consider the original bath state to be initially in the zero-temperature vacuum state $|0_B\rangle$, which translates directly to the no-excitation initial state of $|0_A\rangle \otimes |0_W\rangle$ for the single bosonic mode and the fictitious white reservoir [38], where $|0_A\rangle$ and $|0_W\rangle$ are, respectively, the vacuum states of the single mode and the fictitious white reservoir. The exact master equation of Eq. (45) in Ref. [36] was derived using only the condition

that the reservoir is initially in the zero-temperature vacuum state, from which the reservoir's subsequent evolution to states different from the initial vacuum state can be determined, and finally, the degrees of freedom of the reservoir are averaged over without any approximation to yield the exact master equation.

It was also shown in Ref. [36] that if the reservoir correlation function denoted as $\alpha_{\text{CF}}(t - s)$ is replaced by a δ function, $\alpha_{\text{CF}}(t - s) = \sum_\lambda |g_\lambda|^2 e^{-i\omega_\lambda(t-s)} = \gamma\delta(t - s)$, with some constant γ, then the exact master equation, (36) or (45), presented in Ref. [36] becomes Lindblad's master equation in the standard Markov limit. In our case here, the fictitious white reservoir starts with a reservoir vacuum state $|0_W\rangle$ and has a correlation function delta correlated in time as in Eq. (18). The constant γ used in the correlation function in Ref. [36] equals twice the width Γ here, i.e., $\gamma \to 2\Gamma$. As a result, we obtain the exact master equation for the qubit and the single mode here as

$$\frac{d\tilde{\rho}}{dt}(t) = \frac{1}{i}[H_{\text{Rabi}}, \tilde{\rho}(t)] - \Gamma[a^\dagger a\tilde{\rho}(t) + \tilde{\rho}(t)a^\dagger a - 2a\tilde{\rho}(t)a^\dagger]. \tag{19}$$

Here the qubit–single-mode coupling Hamiltonian

$$H_{\text{Rabi}} = \frac{\Delta}{2}\sigma_z + \omega_0 a^\dagger a + g\sigma_x(a + a^\dagger), \tag{20}$$

without the RW approximation, is the single-mode version of the spin-boson Hamiltonian H_{tot} of Eq. (3).

The presence of the Zeno measurements, considered as a series of repeated projections on the qubit system, does not affect the derived form of the master equation, (19), when the degrees of freedom of the fictitious white reservoir are traced out or averaged over [36]. In fact, expressing the projector $\mathcal{P}_S = e^{-\mu(I-\mathcal{P}_S)}$ with identity operator I and parameter $\mu \to +\infty$ [39], we can combine the dissipative evolution with the projective measurement process as a whole nonunitary dynamics by adding an extra anticommutator bracket term of $-\mu C(t)\{1 - \mathcal{P}_S, \rho\}$, where $C(t) = \sum_{n=0}^\infty \delta(t - n\tau)$ represents a Dirac-comb function. In this representation of Eq. (19), the dissipative single (cavity) mode plays the role of the original bath with a memory time of about $1/\Gamma$, and the initial system-bath state changes from the original bath state $|0_B\rangle$ of $\rho_{\text{tot}}(0) = \mathcal{P}_S \otimes |0_B\rangle\langle0_B|$ to the single-mode state $|0_A\rangle$ of $\tilde{\rho}(0) = \mathcal{P}_S \otimes |0_A\rangle\langle0_A|$.

We emphasize again that we, by no means, make the RW approximation on the qubit-bath coupling Hamiltonian in obtaining Eq. (19), even though the exact decomposition of the original bath involves the RW coupling form of a single mode to a white reservoir [34]. Furthermore, the exact master equation uses only the condition that the original bath with a Lorentzian bath spectral density is initially in the zero-temperature vacuum state or, equivalently, the fictitious white reservoir with the δ-correlated-in-time correlation function is initially in its zero-temperature equilibrium state, i.e., its vacuum state $|0_W\rangle$. Lindblad's master equation (19), which has the same form as a second-order Markovian master equation, is an exact consequence of the model considered here, rather than a second-order Markovian approximation that assumes the reservoir correlation time is very short (but not exactly 0,

i.e., the correlation function is not really delta correlated in time) compared to the other time scales.

As a result, the evolution within a Zeno interval, $(n-1)\tau < t < n\tau$, is then determined by Eq. (19), and at $t = n\tau$ the evolution is described by the projective measurement on the system,

$$
\begin{aligned}
\tilde{\rho}(t^+) &= \mathcal{P}_S \tilde{\rho}(t^-) \mathcal{P}_S \\
&= \mathcal{P}_S \otimes \langle \psi_S | \tilde{\rho}(t^-) | \psi_S \rangle.
\end{aligned} \tag{21}
$$

Equation (21) then serves as the initial state of Eq. (19) for the evolution of the next Zeno interval. This treatment of the dynamics presented here is exact and only the initial condition $\rho_{\text{tot}}(0) = \mathcal{P}_S \otimes |0_B\rangle\langle 0_B|$ is used to derive the exact master equation, even though the Zeno projections violently change the total state from time to time. That the density matrix of the original bath will evolve away from the initial vacuum state $|0_B\rangle\langle 0_B|$ implies that the density matrix of the single mode will evolve away from its initial vacuum state $|0_A\rangle\langle 0_A|$. In addition, the density matrix for the single mode $\langle \psi_S | \tilde{\rho}(t^-) | \psi_S \rangle$ will in general not return to its initial vacuum state $|0_A\rangle\langle 0_A|$ after each measurement. The SP at the final time t is given by $P(t) = \text{Tr}_{S \otimes A} \tilde{\rho}(t)$. In other words, the trace over the bath degrees of freedom (represented here by the degrees of freedom of the single mode) is performed at the end of the final time t. Our treatment reflects the bath memory across different Zeno intervals and leads to interesting dynamical effects.

III. COMPARISON TO PREVIOUS STUDIES

A. Coupling Hamiltonian in the RW approximation

For the population decay model with the coupling Hamiltonian in the RW approximation [25,40,41], if the measurement in action is to determine the SP of the excited state $|e\rangle$ when the initial state is chosen as $|e\rangle \otimes |0_B\rangle$ [8,9], we show next that in this case our master equation gives the same results for the SP as the exact analytical solutions given in Ref. [9].

The total Hamiltonian in the RW approximation reads

$$
H_{\text{RW}} = \frac{\Delta}{2}\sigma_z + \sum_k \omega_k b_k^\dagger b_k + g \sum_k \mu_k (\sigma_+ b_k + \sigma_- b_k^\dagger), \tag{22}
$$

where $\sigma_\pm$ is the qubit creation or annihilation operator, respectively. Suppose the bath is initially in the vacuum state $|0_B\rangle$, then since the total excitation number $N = \sigma_+\sigma_- + \sum_k b_k^\dagger b_k$ of the RW Hamiltonian, Eq. (22), is an invariant quantity [25], the total state at time t for the case of determining the SP in the excited state $|e\rangle$ is within the one-excitation sector and takes the form

$$
|\Psi_{\text{tot}}(t)\rangle = \alpha(t)|e0_B\rangle + \sum_k c_k(t)|g1_k\rangle \tag{23}
$$

with initial conditions $\alpha(0) = 1$ and $c_k(0) = 0$, where $|1_k\rangle = b_k^\dagger|0_B\rangle$ denotes a state with one bath boson (photon) in mode k. The exact solution of the time-dependent coefficient $\alpha(t)$ is given by Eq. (9) in Ref. [9] and reads

$$
\alpha(t) = \frac{1}{2}e^{(i\Delta - i\omega_0 - \Gamma)t/2}(A_+ e^{Dt} + A_- e^{-Dt}), \tag{24}
$$

with $A_\pm = 1 \pm (\Gamma - i\Delta + i\omega_0)/2D$ and $D = \sqrt{\frac{1}{4}(\Gamma - i\Delta + i\omega_0)^2 - g^2}$. So after a Zeno interval τ,

the selective measurement to the qubit excited state projects the total state, Eq. (23), to

$$
|\Psi_{\text{tot}}^M(\tau^+)\rangle = |e\rangle\langle e|\Psi_{\text{tot}}(\tau^-)\rangle = \alpha(\tau)|e0_B\rangle, \tag{25}
$$

where the superscript M denotes that the state to which it is attached is the state right after the measurement, and $\tau^\pm$ denote the times immediately after or before the projective measurement at time τ, respectively. In other words, the (unnormalized) total state returns to its initial form $|e0_B\rangle$ with additional coefficient $\alpha(\tau)$, i.e., with survival probability $P_{\text{RW}}(\tau) = |\alpha(\tau)|^2$. The projective measurement removes the system-bath correlation (entanglement) and the resultant bath state comes back exactly to its initial state $|0_B\rangle$ after each projective measurement to the qubit excited state $|e\rangle$. Thus after n Zeno intervals and n projective measurements to the qubit excited state, one simply gets the (unnormalized) total state $|\Psi_{\text{tot}}^M(n\tau^+)\rangle = \alpha(n\tau)|e0_B\rangle$ with

$$
\alpha(n\tau) = [\alpha(\tau)]^n. \tag{26}
$$

Besides, the survival probability for the qubit to be in the excited state at $t = n\tau^+$ is

$$
\begin{aligned}
P_{\text{RW}}(n\tau) &= \left|\langle e|\Psi_{\text{tot}}^M(n\tau^+)\rangle\right|^2 \\
&= |\alpha(n\tau)|^2 \\
&= [P_{\text{RW}}(\tau)]^n. \tag{27}
\end{aligned}
$$

A comparison of the survival probability $P_{\text{RW}}(t)$ between the above exact analytical solutions [9] and our numerical simulation results using the master equation, Eq. (19), with $H_{\text{Rabi}} \to H_{\text{JC}} = \frac{\Delta}{2}\sigma_z + \omega_0 a^\dagger a + g(\sigma_+ a + \sigma_- a^\dagger)$ for the RW coupling Hamiltonian, is presented in Fig. 1. One can see that they all coincide with each other for different values of the coupling constant g and the spectral density width Γ (the strong-coupling case of $g > 0.6\omega_0$ is also verified, although not shown). In other words, our numerical treatment reproduces exactly the analytical theory of Ref. [9], regardless of how large the qubit-bath coupling strength and the bath correlation time are. This fact demonstrates that our master equation is exact (even though the white-noise dissipative terms look like a standard second-order Markovian Lindblad equation), and thus our master equation approach is a correct and valid tool to study the qubit-bath dynamics in the quantum Zeno process.

Actually only in the above case of determining the SP in the excited state $|e\rangle$ is the result for the SP in the GA the same as that in the KKA [9]. However, if the repeated measurements project the qubit system into an initial general superposition state of $|\psi_S\rangle = \alpha|e\rangle + \beta|g\rangle$ (not just into the initial excited state $|\psi_S\rangle = |e\rangle$), where $|g\rangle$ is the qubit ground state, the bath state after each projective measurement is different. Within the first Zeno interval $0 < t < \tau$, the total state can be written as

$$
|\Psi_{\text{tot}}(t)\rangle = \alpha(t)|e0_B\rangle + \beta(t)|g0_B\rangle + \sum_k c_k(t)|g1_k\rangle, \tag{28}
$$

with the initial condition $\alpha(0) = \alpha$, $\beta(0) = \beta$, and $c_k(0) = 0$. The time-dependent coefficients can still be exactly obtained within the first Zeno interval, with $\alpha(t)$ given by Eq. (24) and $\beta(t) = \beta$. Then the projection of the selective measurement at time
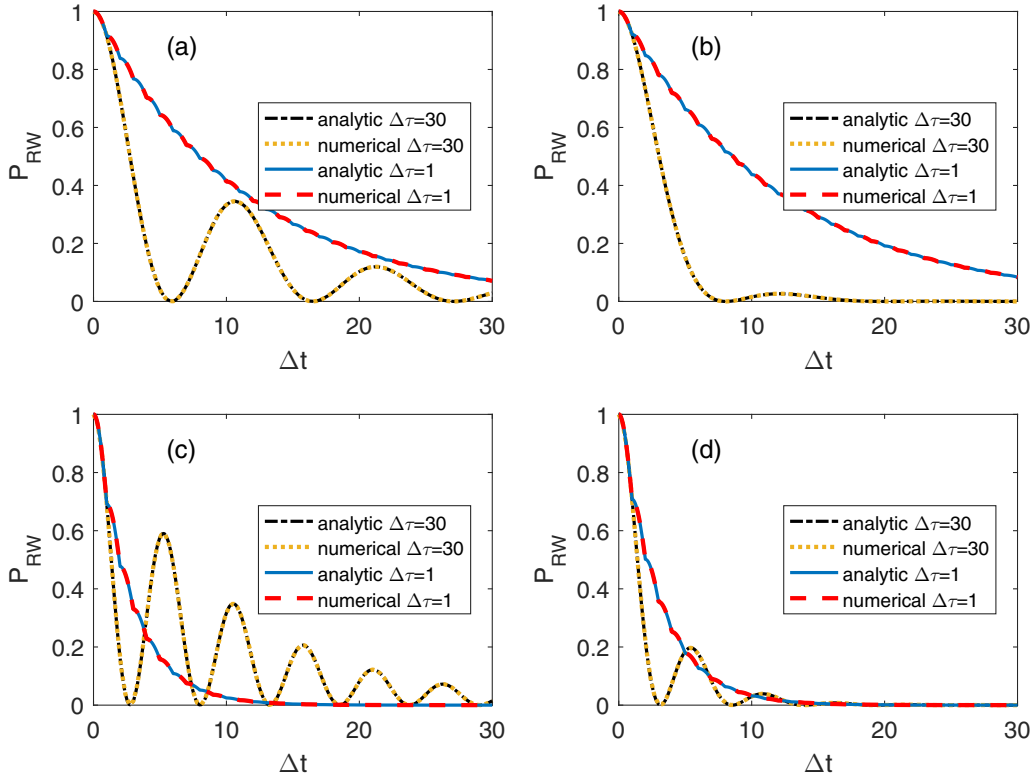
FIG. 1. Survival probabilities as functions of time for $|\psi_S\rangle = |e\rangle$ and $\omega_0 = \Delta$, with the analytical solution from Ref. [9] and the numerical solution from our master equation. (a) $g/\omega_0 = 0.3$, $\Gamma/\omega_0 = 0.1$, (b) $g/\omega_0 = 0.3$, $\Gamma/\omega_0 = 0.3$, (c) $g/\omega_0 = 0.6$, $\Gamma/\omega_0 = 0.1$, and (d) $g/\omega_0 = 0.6$, $\Gamma/\omega_0 = 0.3$.

time τ makes the (unnormalized) bath state

$$\left|\psi_B^M(\tau^+)\right\rangle = \langle\psi_S|\Psi_{\text{tot}}(\tau)\rangle$$
$$= [\alpha^*\alpha(\tau) + |\beta|^2]|0_B\rangle + \beta^* \sum_k c_k(\tau)|1_k\rangle. \quad (29)$$

One clearly sees that this bath state does not return to the initial bath vacuum state $|0_B\rangle$. The SP after the first measurement can be calculated exactly as

$$P_{\text{RW}}(\tau) = \left\langle\psi_B^M(\tau^+)|\psi_B^M(\tau^+)\right\rangle$$
$$= \left|\alpha^*\alpha(\tau) + |\beta|^2\right|^2 + |\beta|^2 \sum_k |c_k(\tau)|^2$$
$$= |\alpha^*\alpha(\tau) + |\beta|^2|^2 + |\beta|^2(|\alpha|^2 - |\alpha(\tau)|^2). \quad (30)$$

However, the (unnormalized) initial total qubit-bath state for the second Zeno interval reads

$$\left|\Psi_{\text{tot}}^M(\tau^+)\right\rangle = |\psi_S\rangle \otimes \left|\psi_B^M(\tau^+)\right\rangle$$
$$= |\psi_S\rangle \otimes [\alpha^*\alpha(\tau) + |\beta|^2]|0_B\rangle$$
$$+ |\beta|^2 \sum_k c_k(\tau)|g\rangle \otimes |1_k\rangle$$
$$+ \beta^*\alpha \sum_k c_k(\tau)|e\rangle \otimes |1_k\rangle, \quad (31)$$

which contains a two-excitation state $|e1_k\rangle$ that goes out the zero-excitation and one-excitation Hilbert space that we set initially for the total-state evolution in the first Zeno interval. Continuing the analysis, one finds that the initial total state for

the evolution of the nth Zeno interval contains n excitations, which is too complex to solve analytically. Thus, we have $P_{\text{RW}}(n\tau) \neq [P_{\text{RW}}(\tau)]^n$ for a general initial qubit state even with the qubit-bath coupling Hamiltonian in the RW approximation. In the following, we still compare the SP in this case between the approximated analytical result $P_{\text{RW}}(n\tau) \approx [P_{\text{RW}}(\tau)]^n$, which assumes that the bath state returns to its initial state after each projective measurement, and that of our master equation in Fig. 2. For the weak-coupling case $g = 0.06$ shown in Figs. 2(a) and 2(b), the approximated results of the KKA [9] agree very well with our exact numerical results, while they deviate from each other in the strong-coupling case $g = 0.6$ as shown in Figs. 2(c) and 2(d). The deviation certainly comes from the changes in the bath state. Therefore, our calculated results demonstrate that the bath state indeed changes in the Zeno projection process in the strong-coupling regime.

B. Coupling Hamiltonian without the RW approximation

For the original spin-boson model without the RW approximation, one cannot obtain an exact solution in the total wave function approach even for the first Zeno interval. References [20,21] are studies of spin or qubit underrepeated nonselective quantum nondemolition (QND) measurements in this model using a perturbation theory for the system-bath coupling strength and assumed the bath to be an immutable entity. The effect of nonselective, nonintrusive QND measurements is to erase the qubit-bath correlation, transforming their joint density matrix into an approximated factorized form. Then
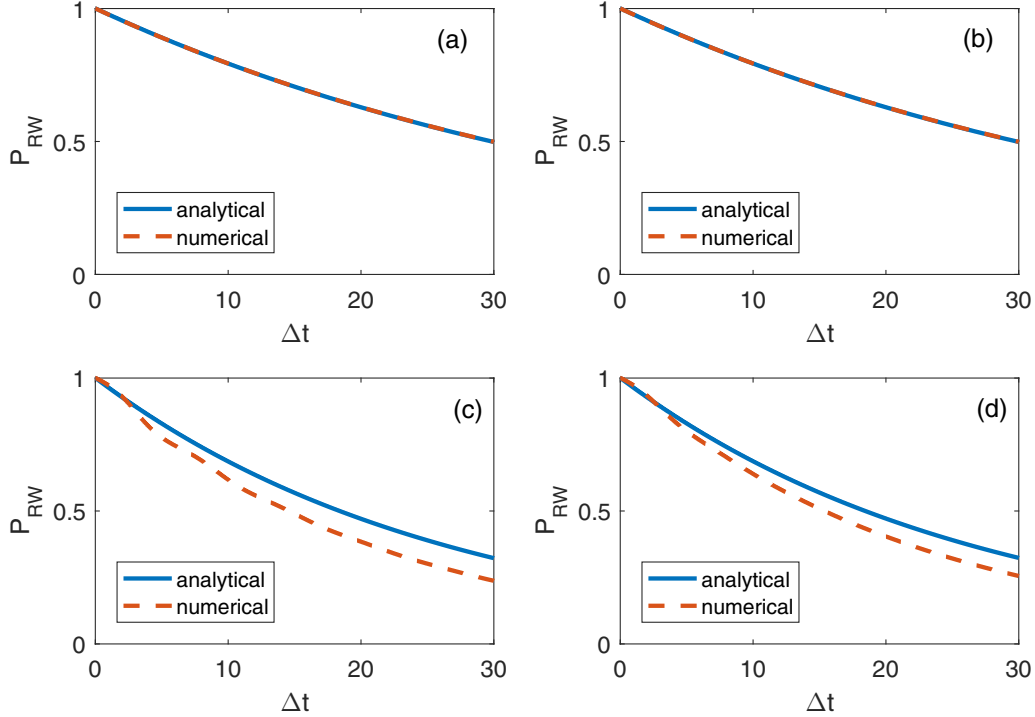
FIG. 2. Survival probabilities as functions of time, with the approximated analytical result and the numerical solution of our master equation, in which the Zeno interval $\Delta\tau = 0.1$, $\omega_0 = \Delta$, and $|\psi_S\rangle = 0.8|e\rangle + 0.6|g\rangle$. (a) $g/\omega_0 = 0.06$, $\Gamma/\omega_0 = 0.1$, (b) $g/\omega_0 = 0.06$, $\Gamma/\omega_0 = 0.3$, (c) $g/\omega_0 = 0.6$, $\Gamma/\omega_0 = 0.1$, and (d) $g/\omega_0 = 0.6$, $\Gamma/\omega_0 = 0.3$.

the reduced density matrix of the qubit remains diagonal throughout the considered evolution and can always be written in Gibbs form, $\rho_S(t) = Z^{-1}e^{-\beta(t)H_S}$, where $\beta(t)$ is the time-dependent effective inverse temperature that characterizes "heating" and "cooling" (cited from Secs. 2.1 and 2.2 in Ref. [21]).

Despite the existing key differences in the measurement scenario and in the measurement effect on the subsequent qubit dynamics, we make comparisons and clarify the validity between the master (rate) equation used in Refs. [20,21] and that used in our work. Taking the zero-temperature system-bath product state $|g0_B\rangle$ as the initial state (which is the same as that in Fig. 1 in Ref. [20]), where $|0_B\rangle$ represents the bath vacuum state, we calculate the excited-state population ρ_{ee} by our master equation following the dynamical rules in Ref. [20]. References [20,21] provided equations of motion of the elements of the reduced density matrix,

$$\frac{d}{dt}\rho_{ee} = -\frac{d}{dt}\rho_{gg} = -R_e\rho_{ee} + R_g\rho_{gg}, \quad (32)$$

with $R_e(t) = 2\int G_0(\omega)\frac{\sin(\omega-\Delta)t}{\omega-\Delta}d\omega$ and $R_g(t) = 2\int G_0(\omega)\frac{\sin(\omega+\Delta)t}{\omega+\Delta}d\omega$. Taking the Lorentzian spectrum to be

$$G_0(\omega) = g^2\frac{1}{\pi}\frac{\Gamma}{(\omega-\omega_0)^2 + \Gamma^2}, \quad (33)$$

we present in Fig. 3 the excited-state population as a function of time given by the two master (rate) equations, namely, Eqs. (19) and (32). One can see that in the weak-coupling regime [Figs. 3(a) and 3(b)], the results obtained by the two master (rate) equations agree well with each other. This demonstrates that our master equation can reproduce the

heating-up behaviors studied in Ref. [20]. However, in cases of moderate coupling [Figs. 3(c) and 3(d)], the results with the two master equations are significantly different in the long-time regime, in which the excited-state population (shown by dashed red lines) given by the master (rate) equation in Refs. [20,21] even falls below 0. This nonphysical result, which is more evident in the strong-coupling regime, indicates that the master (rate) equation in Refs. [20,21] becomes improper to use in these cases, while our exact master equation is still suitable even in the strong-coupling regime.

We note here that in the text of and Supplementary Information to Ref. [20], the postmeasurement bath state and the system-bath correlations are described both analytically and numerically, and in the Supplementary Information to Ref. [21], the small deviation of the bath state from the original Gibbs form is discussed in the weak-coupling perturbation theory, whereas Ref. [22] shows that the bath change is drastic if only a few modes in the bath play a role. These studies [20–22] recognized changes in the bath state, but the effects were argued not to be substantial, due mainly to the fact that many or an infinite number of bath modes were considered and the investigations were conducted within the weak-coupling perturbation theory [20,21]. Using our approach of representing the infinite number of modes of the original Lorentzian bath as a single mode coupled to a fictitious white reservoir of an infinite number of modes, after the infinite number of modes of the white reservoir are traced out, the resultant master equation describes a qubit interacting with effectively a dissipative single mode. When only one bath mode plays a significant role, the results in Refs. [20,21] will also apply to this case of bath changes.
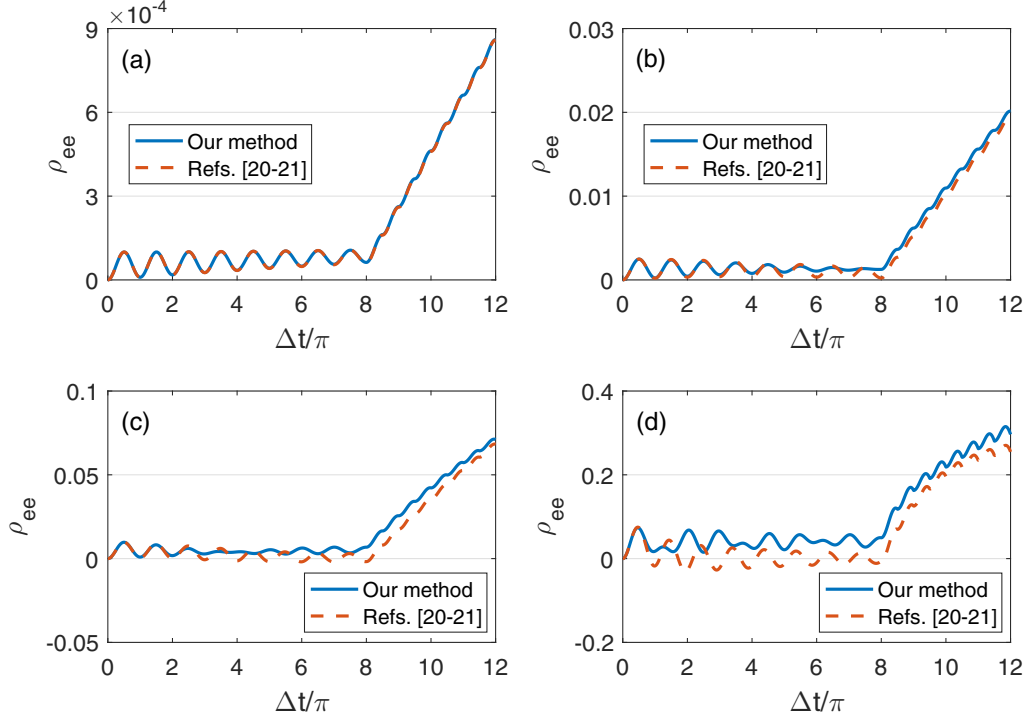
FIG. 3. Excited-level populations given by our master equation (solid blue lines) and the master (rate) equation used in Refs. [20,21] (dashed red lines). The dynamic from $\Delta t = 0$ to $\Delta t = 8\pi$ corresponds to natural relaxation, and for $\Delta t > 8\pi$ it experiences nonselective measurements with interval $\Delta\tau = \pi/2$. Parameters are $\omega_0 = \Delta$, $\Gamma/\Delta = 0.03$. (a) $g/\Delta = 0.01$, (b) $g/\Delta = 0.05$, (c) $g/\Delta = 0.01$, and (d) $g/\Delta = 0.03$.

IV. EFFECTS OF BATH STATE CHANGES AND BATH CORRELATION TIME ON QZE

Next we analyze the properties of the average decay rate in each Zeno interval defined by $\lambda_n = \frac{1}{\tau} \ln\left[P(n\tau)/P(n\tau + \tau)\right]$. As stated, the bath state after a projective measurement for general situations and models is different from the bath state after its previous measurement (i.e., the initial state at the beginning of each Zeno-interval evolution is different), and thus the average decay rates in different Zeno intervals do not equal each other and display rich effects and phenomena. To characterize the changing decay rates between different Zeno intervals, we investigate the behavior of the average decay rate in each interval λ_n. In the KKA (or in the RW-approximated model with projection measurement into $|\psi_S\rangle = |e\rangle$ in Refs. [8,9]), only the total average decay rate $\Lambda_N(\tau) = -\ln P(N\tau)/N\tau$ is used due to the assumption (fact) that the bath state does not change from its initial state and the average decay rates in different Zeno intervals are the same (i.e., the total average decay rate equals the average decay rate in a single Zeno interval). Furthermore, the QZE ($\lambda_n \to 0$ as $\tau \to 0$) indicates $\lambda_n \propto \tau$ for small τ, so it is natural to define their ratio $w_n = \lambda_n/\tau$ as a meaningful and significant physical quantity to characterize the general QZE. We call w_n the scaled decay rate in unit Zeno interval. In the limiting case of continuous Zeno measurements in which $\tau \to 0$, the ratio w_n is actually finite and the discrete series w_n becomes a continuous function of time, namely,

$$\lim_{\tau \to 0, n\tau \to t} (\lambda_n/\tau) = w(t),$$

and the SP takes the form of

$$P(t) = \exp\left[-\tau \int_0^t w(t')dt'\right]. \qquad (34)$$

When $w(t)$ is a constant, the decay is exponential. But if $w(t)$ varies explicitly with time, the decay is nonexponential. $w(t)$ in the KKA is always a constant. Thus in the Zeno limit $\tau \to 0$, the SP always shows exponential-decay behavior in the KKA, but the SP in the GA can still exhibit nonexponential decay. We can derive an analytical expression for the SP in the $\tau \to 0$ limit, which can not only provide us with an understanding of the SP in the very-short-τ regime but also give a verification of the numerical master equation approach. To obtain the explicit analytical expression of $w(t)$ in the $\tau \to 0$ limit, we first directly calculate the total state $|\Psi_{\text{tot}}(t)\rangle$ after n measurements by $|\Psi_{\text{tot}}(t)\rangle = (\mathcal{P}_S e^{-iH_{\text{tot}}\tau})^n |\psi_S 0_B\rangle$. Then obtaining the SP $P(t) = \langle\Psi_{\text{tot}}(t)|\mathcal{P}_S|\Psi_{\text{tot}}(t)\rangle$ to the dominant order in τ and expressing it in the form of Eq. (34), we obtain

$$w(t) = \left\langle H_{S\eta}^2(t)\right\rangle - \langle H_{S\eta}(t)\rangle^2 + g^2(1 - \langle\sigma_x\rangle^2), \qquad (35)$$

where $H_{S\eta}(t) = \Delta\sigma_z/2 + g\sigma_x[\eta(t) + \eta^*(t)]$, and real function

$$\eta(t) = g\langle\sigma_x\rangle[e^{-(\Gamma + i\omega_0)t} - 1]/(\omega_0 - i\Gamma). \qquad (36)$$

This analytical expression of Eqs. (34) and (35), provides a good check for the SP in the small-τ regime calculated by the numerical method of Eqs. (19) and (21).

In Fig. 4, the numerical results of w_n along with the analytical result $w(t)$ are presented for repeated projections to a general initial system state but different τ, g, and Γ. The series $\{\lambda_n = w_n\tau\}$, which shows an oscillatory behavior as a
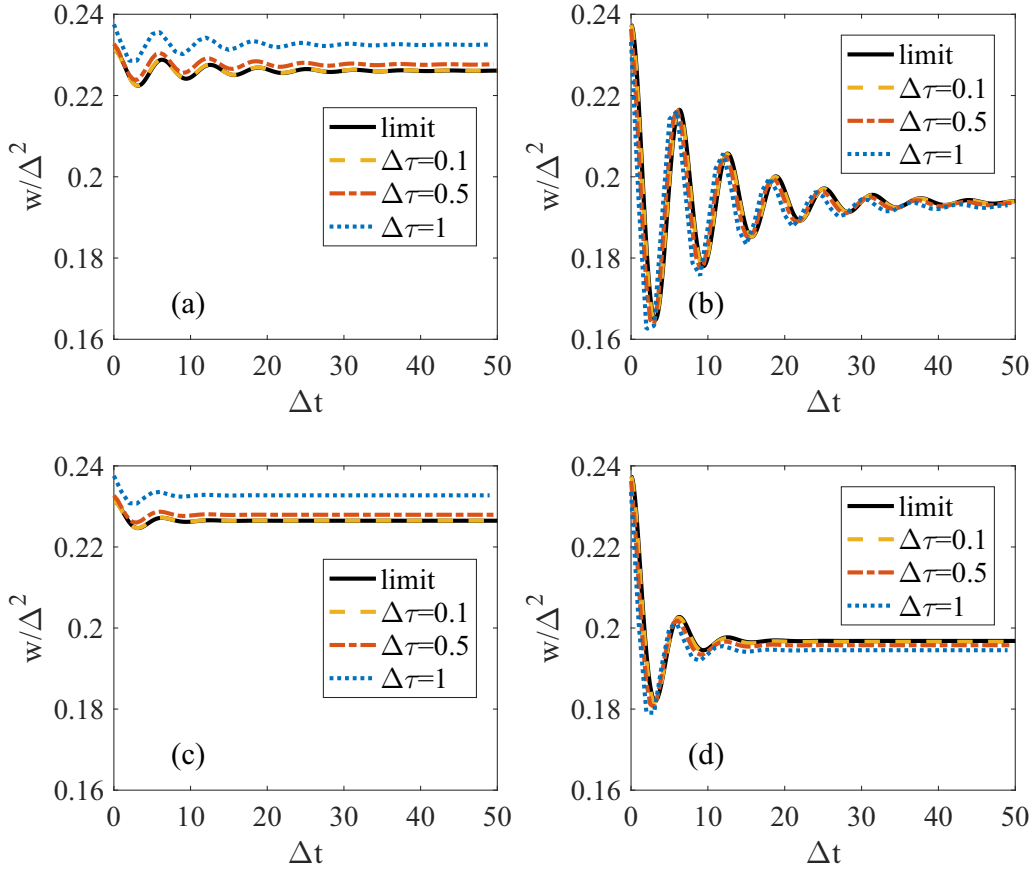
FIG. 4. Scaled decay rates per Zeno interval $w_n = \lambda_n/\tau$ as functions of time t with Zeno interval $\tau = 1/\Delta$ (dotted blue lines), $\tau = 0.5/\Delta$ (dash-dotted red lines), and $\tau = 0.1/\Delta$ (dashed yellow lines) for different values of Γ and g by the numerical solutions. Solid black lines are the analytical results in the continuous limit $\tau \to 0$ from Eq. (35). (a, b) $\Gamma/\Delta = 0.1$; (c, d) $\Gamma/\Delta = 0.3$. (a, c) $g/\Delta = 0.1$; (b, d) $g/\Delta = 0.8$. The initial state is $|\psi_S\rangle = 3/5|e\rangle + 4/5|g\rangle$, where $|e\rangle$ and $|g\rangle$ are the ground and excited states of the qubit, and the parameter $\omega_0/\Delta = 1$. (a) $g/\Delta = 0.1$, $\Gamma/\Delta = 0.1$, (b) $g/\Delta = 0.3$, $\Gamma/\Delta = 0.1$, (c) $g/\Delta = 0.1$, $\Gamma/\Delta = 0.3$, and (d) $g/\Delta = 0.3$, $\Gamma/\Delta = 0.3$.

function of n ($t = n\tau$ for a fixed τ), refers to the variation of the average decay rate across different Zeno intervals, which is significantly different from the oscillatory behavior of the SP (not in the average decay rate) over time t obtained by the KKA or presented in Refs. [8,9], in which the average decay rate in each Zeno interval is a constant. The numerical results for short $\tau = 0.1/\Delta$ (dashed yellow lines) agree quite well with the analytical ones (solid black lines). Besides, $w(t)$ exhibits a damped oscillation with time, indicating that the scaled average decay rate in unit τ for a general initial state is qualitatively different from the constant average decay rate of the traditional QZE.

Furthermore, Fig. 4 presents the quantitative effects of the bath central frequency ω_0, the qubit-bath coupling strength g, and the bath memory time $1/\Gamma$ on the nonexponential decay of $P(t)$ through the behavior of $w(t)$. In each panel, $w(t)$ clearly exhibits damped oscillations because $w(t)$ of Eq. (35) contains both $\eta(t) + \eta^*(t)$ and its square term, with damped oscillation frequencies ω_0 and $2\omega_0$, respectively. Since the $2\omega_0$ term is proportional to g^4, its contribution is much less than the ω_0 term, which is proportional to g^2 for low coupling strengths. Thus the $2\omega_0$ component visible in Fig. 4(b) is not seen in Fig. 4(a). Moreover, as g decreases from Figs. 4(b) to 4(a) as well as from Figs. 4(d) to 4(c), the amplitudes of the

damped oscillations also decrease. This indicates that for very weak system-bath coupling in the KKA, assuming that the bath state does not change significantly from its original state can be justified [20–22]. Figure 4 also shows the influence of Γ on the damping behavior of $w(t)$. The damping rate of $w(t)$ is, as shown in Eq. (36), just the width Γ of the Lorentzian spectrum, namely, the dissipation rate of the single (cavity) mode, whose inverse value $1/\Gamma$ characterizes the memory time of the Lorentzian bath. When $\Gamma = 0$, the qubit is effectively coupled to a single mode and exchanges information with it periodically. As a result, $w(t)$ oscillates without damping. For finite values of Γ, if the evolution time t is much longer than the memory time $1/\Gamma$, then $w(t)$ will approach a constant value just like the traditional QZE.

The analytical result of w_{KKA} in the continuous limit $\tau \to 0$ in the KKA can be found by $w_{\text{KKA}} = \langle\Psi_{\text{tot}}(t)|H_{\text{tot}}^2|\Psi_{\text{tot}}(t)\rangle - \langle\Psi_{\text{tot}}(t)|H_{\text{tot}}|\Psi_{\text{tot}}(t)\rangle^2 = (\Delta/2)^2(1 - \langle\sigma_z\rangle^2) + g^2$ [8]. For finite Zeno interval τ, we can express the SP $P_{\text{KKA}}(\tau)$ associated with one measurement in the KKA as $P_{\text{KKA}}(\tau) = |\langle\psi_S 0_A|e^{-iH_{\text{eff}}\tau}|\psi_S 0_A\rangle|^2$, where $H_{\text{eff}} = H_{\text{Rabi}} - i\Gamma a^\dagger a$ is the effective non-Hermitian Hamiltonian, which takes into account the single-mode decay [34,42]. The result of w_{KKA} for finite τ can thus be obtained by $w_{\text{KKA}} = -\frac{1}{\tau^2}\ln P_{\text{KKA}}(\tau)$, with the dynamics of $P_{\text{KKA}}(\tau)$ solved numerically. The comparisons
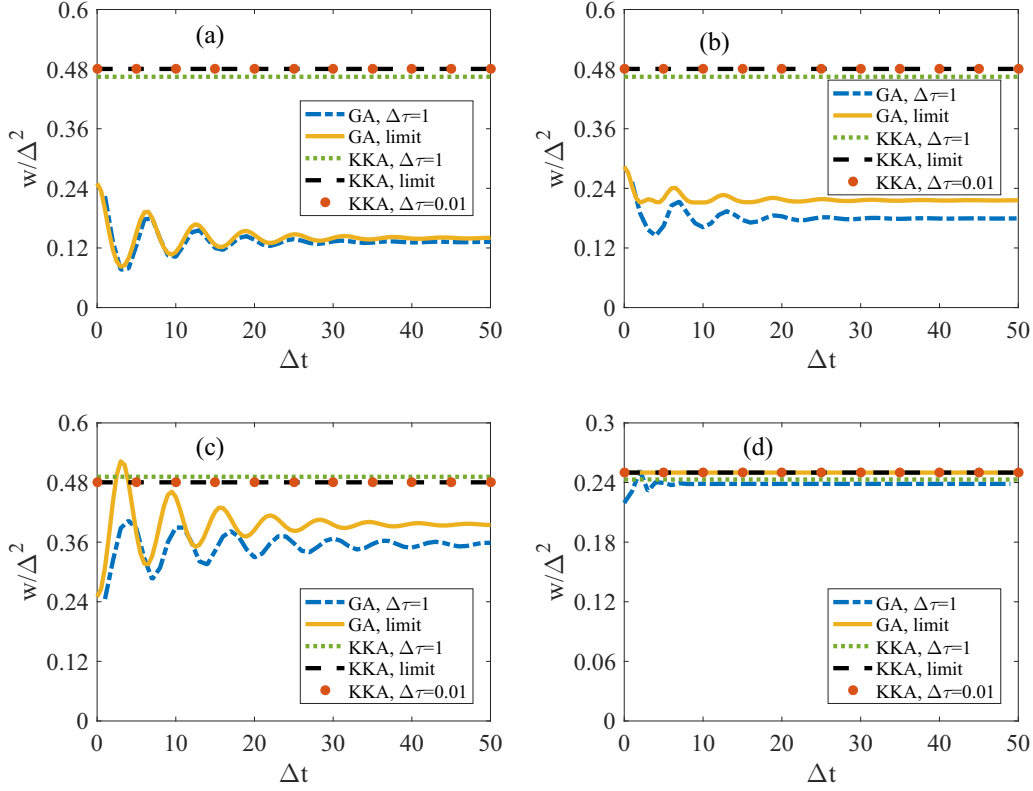
FIG. 5. Functions $w(t)$ and constants w_{KKA} for different initial states of $|\psi_S\rangle = \alpha|e\rangle + \beta|g\rangle$, with (α,β) equal to (a) (3/5,4/5), (b) $(3/5,e^{i\pi/8}4/5)$, (c) (4/5,3/5), and (d) (1,0). The results of $w(t)$ for $\tau = 1/\Delta$ (dash-dotted blue lines) are calculated numerically using Eqs. (19) and (21), and for the continuous limit $\tau \to 0$ (solid yellow lines) the results are calculated analytically using Eq. (35). The results of w_{KKA} for $\tau = 1/\Delta$ (dotted green lines) as well as $\tau = 0.01/\Delta$ (small red circles) are calculated numerically, and for the continuous limit $\tau \to 0$ (dashed black lines) the results are calculated analytically using the formulas in the KKA described in the text. Other parameters used are $\omega_0/\Delta = 1$, $g/\Delta = 0.5$, and $\Gamma/\Delta = 0.1$. (a) $(\alpha,\beta) = (3/5,4/5)$ (b) $(\alpha,\beta) = (3/5,4e^{i\pi/8}/5)$ (c) $(\alpha,\beta) = (4/5,3/5)$, and (d) $(\alpha,\beta) = (1,0)$.

between functions $w(t)$ and constants w_{KKA} for the same parameters but different values of τ are presented in each panel in Fig. 5. One can see that the numerical results of w_{KKA} for $\Delta\tau = 0.01$ (small red circles) agree well with the analytical results of w_{KKA} for $\tau \to 0$ (dashed black lines), which again verifies the single-mode approach used in this paper. Compared to w_{KKA}, the function $w(t)$, taking account of the cross-correlation of the bath operators between different Zeno intervals and the bath memory time, exhibits rich phenomena. The SP right after the first Zeno measurement in the GA is always larger than or equal to that in the KKA since $P(\tau) = \text{Tr}_B\langle\psi_S|\rho_{\text{tot}}(\tau)|\psi_S\rangle \geqslant \langle 0_B|\langle\psi_S|\rho_{\text{tot}}(\tau)|\psi_S\rangle|0_B\rangle = P_{\text{KKA}}(\tau)$. Note, again, that in the Zeno limit $\tau \to 0$, w_{KKA} is a constant but $w(t)$ shows damped oscillation behavior for general initial states. The constant w_{KKA}, by means of Eq. (34), leads to the exponential-decay SP $P(t) = e^{-\tau w_{\text{KKA}}t}$ ($w_{\text{KKA}}^{-1/2}$ is just the Zeno time). Therefore, the fact that the SP of a general initial qubit state in the regime of very small Zeno intervals shows exponential-decay behavior in the KKA, but shows nonexponential decay in our GA, is also an important major difference between these two approaches, even though at large Zeno time intervals the different approaches may all show damped oscillatory behaviors in the SP. Depending on the initial states and the value of τ, $w(t)$ can then, as shown in Fig. 5, be greater or less than w_{KKA}.

Moreover, the relative phase between the basis states of $|e\rangle$ and $|g\rangle$ of the initial qubit state $|\psi_S\rangle = \alpha|e\rangle + \beta|g\rangle$ has [compare Fig. 5(a) with Fig. 5(b)] an important effect on $w(t)$. In contrast, the KKA results near the continuous limit do not depend on the relative phase in the initial state, for the initial phase is not explicitly contained in the expression of w_{KKA}. In fact, in the model investigated, w_{KKA} in the continuous limit depends only on $1 - \langle\sigma_z\rangle^2$, so w_{KKA} is the same for the particularly chosen different initial states in Figs. 5(a)–5(c). In Fig. 5(d), the scaled decay rates $w(t)$ in the continuous limit $\tau \to 0$ (solid yellow line) is a constant and equals w_{KKA} (dashed black line), i.e., $w(t) = w_{\text{KKA}} = g^2$. This is because the initial state $|\psi_S\rangle = |e\rangle$ makes $\langle\sigma_x\rangle = 0$ and thus according to Eq. (36) the amplitudes of the oscillation parts of $w(t)$ are 0. But for finite Zeno interval τ, w_n still oscillates with time (dash-dotted blue line), attributed to the higher-order effect of the finite value of τ.

V. TRANSITION BETWEEN THE QZE AND THE QAZE

Next we discuss the transition between the QZE and the QAZE. It is known that a longer Zeno interval may lead to the QAZE. In the KKA, the total average decay rate $\lambda_{\text{KKA}}(\tau) = -\ln P(t)/t = -\ln P(\tau)/\tau$ depends only on τ and is independent of the number of measurements N. One may
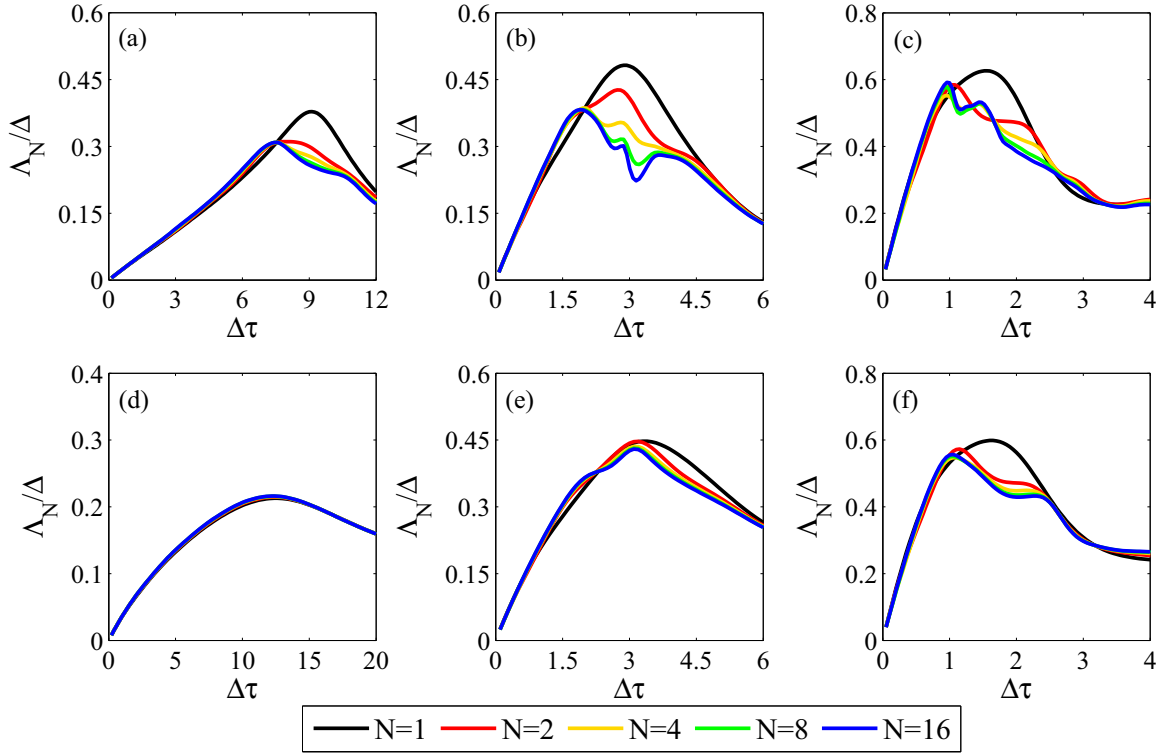
FIG. 6. Total average decay rate Λ_N as a function of the Zeno interval τ for various numbers of measurements N. (a–c) The width is $\Gamma/\Delta = 0.1$; (d–f) $\Gamma/\Delta = 0.3$. The coupling strength is $g/\Delta = 0.2$ in (a) and (d), $g/\Delta = 0.5$ in (b) and (e), and is $g/\Delta = 0.9$ in (c) and (f). Black, red, yellow, green, and blue lines correspond to $N = 1, 2, 4, 8,$ and 16, respectively. The initial state is $|\psi_S\rangle = |e\rangle$ and the other parameter used is $\omega_0/\Delta = 1$. (a) $\Gamma/\Delta = 0.1, g/\Delta = 0.2$, (b) $\Gamma/\Delta = 0.1, g/\Delta = 0.5$, (c) $\Gamma/\Delta = 0.1, g/\Delta = 0.9$, (d) $\Gamma/\Delta = 0.3, g/\Delta = 0.2$ (e) $\Gamma/\Delta = 0.3, g/\Delta = 0.5$, and (f) $\Gamma/\Delta = 0.3, g/\Delta = 0.9$.

define $\frac{d}{d\tau}\lambda_{\text{KKA}}(\tau) > 0$ as the QZE and $\frac{d}{d\tau}\lambda_{\text{KKA}}(\tau) < 0$ as the QAZE, with the QZE-QAZE transition point called the transition time τ^c [8,14–17]. As we have seen, the decay rate per Zeno interval λ_n or scaled decay rate w_n varies also with the number of measurements. Thus the QZE-AZE transition point should depend also on the number of measurements N [16]. The total average decay rate, $\Lambda_N(\tau)$, for N measurements is defined as $\Lambda_N(\tau) = -\ln P(N\tau)/N\tau = \frac{1}{N}\sum_{n=0}^{N-1}\lambda_n$. For each given N, we define $\frac{d}{d\tau}\Lambda_N(\tau) > 0$ as the QZE and $\frac{d}{d\tau}\Lambda_N(\tau) < 0$ as the QAZE, with the transition time τ_N^c given by the transition points. This definition for the transition between QZE and QAZE is a straightforward extension of the traditional definition, i.e., for $N = 1$, it goes back to the traditional definition.

The total average decay rates $\Lambda_N(\tau)$ as functions of τ with initial state $|\psi_S\rangle = |e\rangle$ for various N's presented in Fig. 6 are different from each other, and for each N there is a corresponding transition time τ_N^c. This is qualitatively different from the traditional QZE-QAZE transition. As N increases, the transition time τ_N^c becomes smaller. This may lead to an interesting result. For example, in Fig. 6(b), the transition point for $N = 1$ (black line) is near $\tau = 3/\Delta$, while those for $N = 8$ and 16 (green and blue lines, respectively) are close to $\tau = 2/\Delta$. If the Zeno interval is set to be fixed at $\tau = 2.5/\Delta$, then the KKA ($N = 1$) would predict a QZE, while the general approach predicts a qualitatively different QAZE for large-N measurements. Besides, the blue curves in Figs. 6(b) and 6(c) show multiple transition

points, which might be regarded as multiple QZE-QAZE transitions [16].

The parameters Γ and g also have significant effects on the transition between the QZE and the QAZE. In Figs. 6(a)–6(c), with a small width, $\Gamma/\Delta = 0.1$, the curves for various N's separate from one another, while in Figs. 6(d)–6(f), with a larger width, $\Gamma/\Delta = 0.3$, the curves almost overlap one another. One can also observe that the curves of various N's deviate from one another in the strong-coupling regime [Figs. 6(c) and 6(f)] but are close to one another in the weak-coupling regime [Figs. 6(a) and 6(d)]. In the regime of large Γ (short bath correlation time) and small g (weak coupling), as in Fig. 6(d), all the curves for different N's tend to overlap one another, and the QZE and QAZE behaviors approach those of the KKA.

VI. CONCLUSION

In summary, we have investigated the influence of the bath memory effect on the QZE and QAZE. The assumption that the bath state resets to its original state after each instantaneous projective measurement on the system in the traditional approach ignores equivalently the cross-correlations of the bath operators at different Zeno intervals. For measurements projected to a general initial system state and for a bath with a considerable memory effect, the assumption is not valid. To solve the dynamics, we derive an exact master equation for a Lorentzian bath which is suitable for the case where the qubit system undergoes time-dependent nonunitary operations

such as Zeno projections, and we compare it with former methods for verification. Based on the exact result we find that, in stark contrast to the behaviors found in the KKA, the scaled average decay rates in unit Zeno interval w_n in our GA display an oscillatory behavior, enabling, even in the regime of very small Zeno intervals, a nonexponential decay behavior in the SP, and the total average decay rate depends not only on τ but also on the number of repeated measurements N. For a fixed N, some values of τ for which the traditional approach predicts a QZE region may in fact already be in the QAZE region. Overall, the width Γ characterizes the damping rate of the memory and the system-bath coupling strength g characterizes the memory depth of the bath. So small Γ and large g make the cross-correlation between different Zeno intervals substantially nonnegligible, resulting in significant quantitative as well as qualitative differences between the GA and the KKA. Our results provide an essential step toward

a further in-depth and comprehensive understanding of the complex problems of the QZE and QAZE in open quantum systems. It will be interesting to see whether our predictions can be verified experimentally in realistic systems such as superconducting circuit QED systems.

[1] B. Misra and E. C. G. Sudarshan, J. Math. Phys. **18**, 756 (1977).

[2] D. Home and M. B. A. Whitaker, Ann. Phys. (NY) **258**, 237 (1997).

[3] W. M. Itano, D. J. Heinzen, J. J. Bollinger, and D. J. Wineland, Phys. Rev. A **41**, 2295 (1990).

[4] E. W. Streed, J. Mun, M. Boyd, G. K. Campbell, P. Medley, W. Ketterle, and D. E. Pritchard, Phys. Rev. Lett. **97**, 260402 (2006).

[5] C. Search and P. R. Berman, Phys. Rev. Lett. **85**, 2272 (2000).

[6] H. Zheng, S. Y. Zhu, and M. S. Zubairy, Phys. Rev. Lett. **101**, 200404 (2008).

[7] S. Maniscalco, F. Francica, R. L. Zaffino, N. Lo Gullo, and F. Plastina, Phys. Rev. Lett. **100**, 090503 (2008).

[8] A. G. Kofman and G. Kurizki, Nature (London) **405**, 546 (2000).

[9] A. G. Kofman and G. Kurizki, Phys. Rev. A **54**, R3750 (1996).

[10] M. C. Fischer, B. Gutierrez-Medina, and M. G. Raizen, Phys. Rev. Lett. **87**, 040402 (2001).

[11] P. Facchi, H. Nakazato, and S. Pascazio, Phys. Rev. Lett. **86**, 2699 (2001).

[12] S. Maniscalco, J. Piilo, and K.-A. Suominen, Phys. Rev. Lett. **97**, 130402 (2006).

[13] Q. Ai, Y. Li, H. Zheng, and C. P. Sun, Phys. Rev. A **81**, 042116 (2010).

[14] D. Segal and D. R. Reichman, Phys. Rev. A **76**, 012109 (2007).

[15] A. Thilagam, J. Phys. A: Math. Theor. **43**, 155301 (2010).

[16] A. Z. Chaudhry and J. B. Gong, Phys. Rev. A **90**, 012101 (2014).

[17] A. Z. Chaudhry, Sci. Rep. **6**, 29497 (2016).

[18] I. Lizuain, J. Casanova, J. J. García-Ripoll, J. G. Muga, and E. Solano, Phys. Rev. A **81**, 062131 (2010).

[19] X. Cao, Q. Ai, C. P. Sun, and F. Nori, Phys. Lett. A **376**, 349 (2012).

[20] N. Erez, G. Gordon, M. Nest, and G. Kurizki, Nature **452**, 724 (2008).

[21] G. Gordon, G. Bensky, D. Gelbwaser-Klimovsky, D. D. B. Rao, N. Erez, and G. Kurizki, New J. Phys. **11**, 123025 (2009).

[22] G. A. Álvarez, D. D. Bhaktavatsala Rao, L. Frydman, and G. Kurizki, Phys. Rev. Lett. **105**, 160401 (2010).

[23] Another commonly seen formula through which the SP $P_{\text{KKA}}(\tau)$ right after a single projective measurement ($N = 1$) is calculated in many QZE and QAZE studies in the KKA is $P_{\text{KKA}}(\tau) = \text{Tr}_{S \otimes B}[\mathcal{P}_S U(\tau) \rho_{\text{tot}}(0) U^\dagger(\tau) \mathcal{P}_S]$, but then the assumption that the

bath is reset to its initial state $\rho_B(0)$ is implicitly made so that the total system-bath evolution in the next Zeno interval is the same as that in the previous interval, and consequently $P_{\text{KKA}}(t) = [P_{\text{KKA}}(\tau)]^N$.

[24] A. J. Legget *et al.*, Rev. Mod. Phys. **59**, 1 (1987).

[25] H. P. Breuer and F. Petruccione, *The Theory of Open Quantum Systems* (Oxford University Press, Oxford, UK, 2002).

[26] A. Blais, R.-S. Huang, A. Wallraff, S. M. Girvin, and R. J. Schoelkopf, Phys. Rev. A **69**, 062320 (2004).

[27] A. Wallraff, D. I. Schuster, A. Blais, L. Frunzio, R.-S. Huang, J. Majer, S. Kumar, S. M. Girvin, and R. J. Schoelkopf, Nature **431**, 162 (2004).

[28] M. Sarovar, H.-S. Goan, T. P. Spiller, and G. J. Milburn, Phys. Rev. A **72**, 062327 (2005); S.-Y. Huang, H.-S. Goan, X. Q. Li, and G. J. Milburn, *ibid.* **88**, 062311 (2013).

[29] R. J. Schoelkopf and S. M. Girvin, Nature **451**, 664 (2008); S. M. Girvin, M. H. Devoret, and R. J. Schoelkopf, Phys. Scr. **T137**, 014012 (2009).

[30] J. Q. You and F. Nori, Nature **474**, 589 (2011).

[31] M. O. Scully and M. S. Zubairy, *Quantum Optics* (Cambridge University Press, Cambridge, UK, 1997).

[32] C. Wang and Q. H. Chen, New J. Phys. **15**, 103020 (2013).

[33] B. M. Garraway, Phys. Rev. A **55**, 2290 (1997); **55**, 4636 (1997).

[34] Z. X. Zhou, Z. G. Lü, and H. Zheng, Quantum Inf. Process. **15**, 3223 (2016).

[35] M. Rosenau da Costa, A. O. Caldeira, S. M. Dutra, and H. Westfahl, Jr., Phys. Rev. A **61**, 022107 (2000).

[36] W. T. Strunz and T. Yu, Phys. Rev. A **69**, 052115 (2004).

[37] T. Yu, Phys. Rev. A **69**, 062107 (2004).

[38] Q.-J. Tong, J.-H. An, H.-G. Luo, and C. H. Oh, Phys. Rev. B **84**, 174301 (2011).

[39] The operator $e^{-\mu(I-\mathcal{P}_S)} = I + \sum_{n=1}^{\infty} \frac{(-\mu)^n(I-\mathcal{P}_S)^n}{n!}$. Since $(I - \mathcal{P}_S)^n = I - \mathcal{P}_S$ for $n \geqslant 1$, one has $e^{-\mu(I-\mathcal{P}_S)} = \mathcal{P}_S + e^{-\mu}(I - \mathcal{P}_S)$. So $\mathcal{P}_S = e^{-\mu(I-\mathcal{P}_S)}$ when $\mu \to \infty$.

[40] B. Bellomo, R. Lo Franco, and G. Compagno, Phys. Rev. Lett. **99**, 160502 (2007).

[41] J.-S. Tai, K.-T. Lin, and H.-S. Goan, Phys. Rev. A **89**, 062310 (2014).

[42] C. W. Gardiner and P. Zoller, *Quantum Noise*, 2nd ed. (Springer-Verlag, Berlin, 2000).